Studia Geotechnica et Mechanica, Vol. 38, No. 1, 2016
DOI: 10.1515/sgem-2016-0012

THE INFLUENCE OF NORMAL FAULT ON INITIAL STATE OF STRESS IN ROCK MASS

ANTONI TAJDUŚ, MAREK CAŁA

AGH University of Science and Technology in Cracow, Poland

KRZYSZTOF TAJDUŚ

Strata Mechanics Research Institute, Polish Academy of Sciences in Cracow, Poland,
e-mail: tajdus@img-pan.krakow.pl

Abstract: Determination of original state of stress in rock mass is a very difficult task for rock mechanics. Yet, original state of stress in rock mass has fundamental influence on secondary state of stress, which occurs in the vicinity of mining headings. This, in turn, is the cause of the occurrence of a number of mining hazards, i.e., seismic events, rock bursts, gas and rock outbursts, falls of roof. From experience, it is known that original state of stress depends a lot on tectonic disturbances, i.e., faults and folds. In the area of faults, a great number of seismic events occur, often of high energies. These seismic events, in many cases, are the cause of rock bursts and damage to the constructions located inside the rock mass and on the surface of the ground. To estimate the influence of fault existence on the disturbance of original state of stress in rock mass, numerical calculations were done by means of Finite Element Method. In the calculations, it was tried to determine the influence of different factors on state of stress, which occurs in the vicinity of a normal fault, i.e., the influence of normal fault inclination, deformability of rock mass, values of friction coefficient on the fault contact. Critical value of friction coefficient was also determined, when mutual dislocation of rock mass part separated by a fault is impossible. The obtained results enabled formulation of a number of conclusions, which are important in the context of seismic events and rock bursts in the area of faults.

Key words: *underground mining, stress field , tectonic disturbances, fault, rock burst, seismic events*

1. INTRODUCTION

Fault is a structure created as a result of original continuity break of rocks and their dislocation along the fault surface. From the mechanical point of view, fault is a discontinuity which has influence on state of stress, deformability of rock and its displacements, thus it makes mining difficult in its surroundings. Generally, it was found that existence of faults:

- causes disturbance of state of stress in their surroundings which create places of concentration and relief of stresses. As far as seismic events and rock bursts are concerned, the places of stress concentration are dangerous where unfavorable accumulation of energy appears;
- causes generation of seismic events of high energy, in the case of regional/local faults and big throws. The highest energies of seismic events are connected with dislocations along the fault (usually on certain sections of fault surface), which can appear as a result of mining seams of significant thickness at one or the other side of the fault (particularly an irregular one), reduce of friction value on the fault contact (e.g., by decreasing forces perpendicular to fault surface, which are the result of mining in the area of fault);
- limit the size of mining panels (create a natural boundary for a mining panels). It refers mainly to faults with mean and big throws, as a rule with known traces;
- causes difficulties while mining. Faults with slight throws lead to irregular run of longwalls, the necessity of waste rock ripping in the roof or floor and, sometimes "askew" the longwall.

Disturbance degree of initial state of equilibrium caused by the fault occurrence depends on a number of factors, of which the most significant are:

– angle of dip (inclination) of fault plane,
– angle of friction on the fault plane,
– size of throw,
– diversification of geological structure and properties of rocks, particularly deformability of rocks (value of Young's modulus and Poisson's ratio).

In order to get answers to some of the questions, numerical calculations were done. The calculations were to answer the following questions:

a) How does state of stress change as a result of normal fault occurrence?
b) What is the influence of normal fault inclination on state of stress?
c) How do rock mass properties influence state of stress?
d) From what critical value of friction coefficient on the fault contact, characteristic of a given inclination of fault surface and deformability of rocks, is mutual dislocation of part of rock mass separated by a fault possible, while rock mass behaves as homogeneous, lacking discontinuity?

The answers to these questions are extremely important in the context of seismic events and rock bursts in the area of faults.

2. NUMERICAL CALCULATIONS OF THE INFLUENCE OF FAULT EXISTENCE ON INITIAL STATE OF STRESS IN ROCK MASS, THE FAULT MODELED BY MEANS OF BI-NODAL CONTACT ELEMENTS OF GAP TYPE WITH FRICTION

In order to estimate the influence of fault existence on state of stress in rock mass, numerical calculations were done for six models, which were different from each other with fault dip (Flisiak et al. 2000):

– model 1 – inclination 1.5:1 (56.31°),
– model 2 – inclination 2:1 (63.44°),
– model 3 – inclination 3:1 (71.57°),
– model 4 – inclination 4:1 (75.96°),
– model 5 – inclination 5:1 (78.69°),
– model 6 – inclination 6:1 (80.54°).

To reduce the number of factors influencing the disturbance of initial state of stress, it was assumed that the rock mass is homogeneous, isotropic, linearly-elastic. In that way, the influence of geological structure was eliminated. For the analysed models, the following elastic properties were accepted:

– Young's modulus $E = 5.0$ GPa,
– Poisson's ratio $\nu = 0.25$,
– density 2.5 Mg/m^3.

The numerical model used in calculations was a plate cut in rock mass, 8000 m long and 2000 m high, in the central part where the fault plate was located of the inclination appropriate for a given model (Fig. 1). The calculations were done in 2D, assuming that the fault stretch is infinitely big. On the edges of the models, the following conditions were accepted:

– on vertical edges of the plate – horizontal displacements equal zero,
– on bottom edge of the plate vertical displacements equal zero.

Calculation plate was covered with the mesh of triangular, hexa-nodal finite elements (total number of nods amounted to 22,230). On the surface of discontinuity, bi-nodal contact elements GAP type were intro-

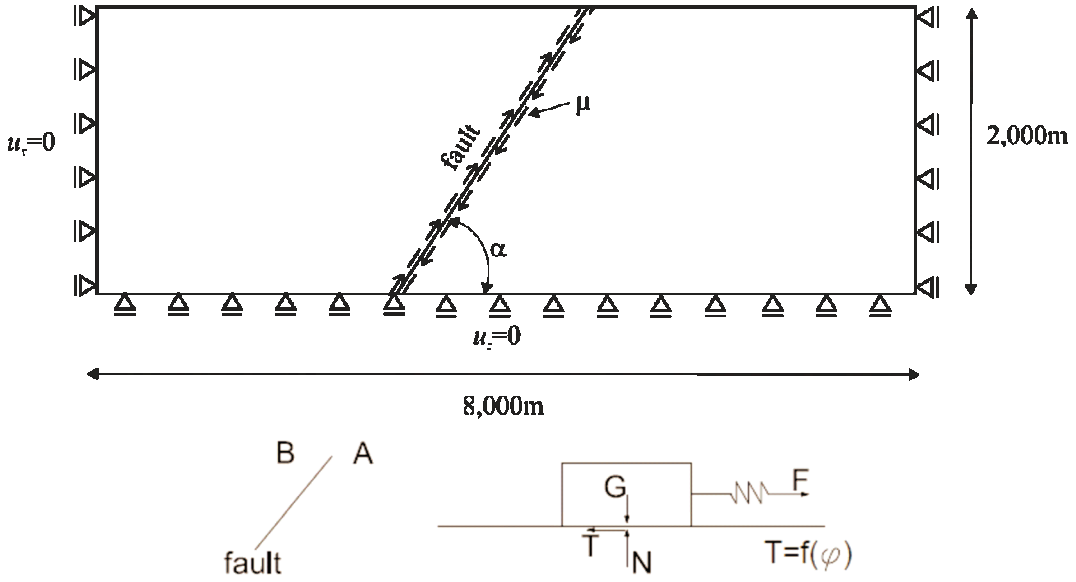

Fig. 1. Calculation plate with model GPA type (below the plate)

duced, enabling independent dislocation to each other of both parts of rock mass.

Calculations for each model mentioned above were done with different values of friction coefficient, starting with zero value for which there was a slip between the parts of the model separated by a fault, up to critical values of friction coefficient, for which there was no slip. Because of the huge volume of the results obtained, only the most interesting ones are discussed in detail below.

For model 1, in which the inclination of the fault to horizontal plate amounted to 1.5:1 (56.31°), the calculations were done for the following values of friction coefficient: $\mu = 0.0$, $\mu = 0.5$, $\mu = 1.0$, $\mu = 1.5$, $\mu = 2.0$, $\mu = 2.1$ (critical value when there was no slip on the fault).

The analysis of the obtained results indicates that the biggest disorder of state of stress and displacement appear in rock mass, in which there is no friction ($\mu = 0.0$), as there is an increase in friction value, the displacement caused by the fault existence decreases and with the friction value when there is no slip, the disorder of initial state of stress and displacement is small. In Fig. 2, the distribution of horizontal stresses at a few depths is presented.

In foot wall, maximum horizontal stresses from the surface up to the depth of about 750 m are tensile (at the depth of 350 m their value reaches 12 MPa). As the depth increases, the stresses decrease and after crossing the depth of 750 m, they change into compressive stresses lower than the value of initial horizontal stress. At a depth of 350 m, maximum stresses are at a distance of about 1,600 m from the fault, as the depth increases, they approach it and at a depth of 1,150 m, they are at a distance of 570 m from the fault.

Horizontal stresses as they approach the fault, rapidly decrease, and in its direct neighbourhood they reach high values of compression, crossing significantly the values of horizontal initial stresses fora given depth. The highest horizontal compression stresses occur on the fault in foot wall at smaller

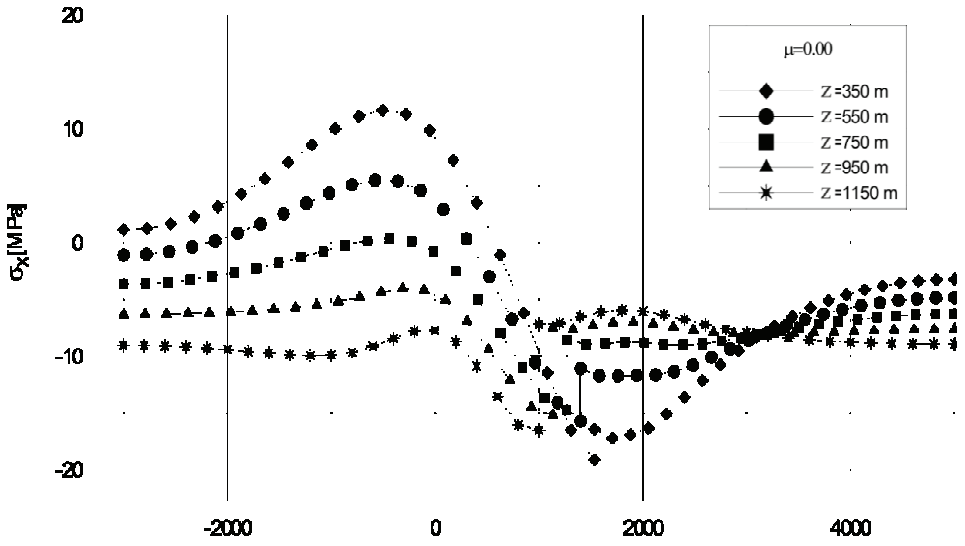

Fig. 2. Distribution of horizontal stresses in fault area with inclination 1.5:1 in no friction case

Table 1. Values of horizontal stresses in a few characteristic places

Inclination of fault 1.5:1 (56.31°), no friction on fault								
Depth H [m]	p_x [MPa]	Zone before fault		On fault				
		$\frac{\sigma_x^{\min}}{p_x}$	Distance of smallest stresses from fault [m]	σ_x in foot wall [MPa]	$\frac{\sigma_x}{p_x}$ Foot wall	σ_x Hanging wall [MPa]	$\frac{\sigma_x}{p_x}$ Hanging wall	Difference of stresses on fault [MPa]
350	–2.9	–4.2	1600	–19.5	6.7	–16.5	5.7	–3
550	–4.6	–1.1	1350	–15.5	3.4	–11.0	2.4	–4.5
750	–6.2	–0.1	1080	–15.0	2.4	–8.5	1.4	–6.5
950	–7.9	0.6	830	–15.0	1.9	–7.5	0.9	–7.5
1150	–9.6	0.8	570	–16.5	1.7	–7.0	0.7	–9.5

depths (e.g., at a depth of 350 m, $\frac{\sigma_x}{p_x} = 6.7$). With the increase of depth, the ratio of horizontal stresses to horizontal initial stresses decreases (at a depth of 1,150 m it amounts to $\frac{\sigma_x}{p_x} = 1.7$).

After coming from foot wall to *hanging wall*, fluctuating variation of horizontal stresses is observed, which increase from 3 MPa at a depth of 350 m, to 9.5 MPa at a depth of 1,150 m. In hanging wall, horizontal stresses are compressive. At small depths, horizontal compressive stresses are repeatedly higher than initial horizontal stresses. As the depth increases, the ratio decreases falling below value 1.0.

In Table 1, values of horizontal stresses in a few characteristic places are shown.

In foot wall vertical stresses are compressive on the whole plate (Fig. 3).

Great disturbances of vertical stresses occur in the vicinity of the fault, and increase with depth. At small depths, in foot wall, vertical stresses change slightly. At bigger depths, while approaching the fault in foot wall, vertical stresses of compressive character increase fast, reaching their extreme value at a distance of 1,000 m from the fault. In the area of fault, while coming from foot wall to hanging wall, big fluctuating fall in stresses (relief) is observed, which is the bigger, the bigger the depth is. At a depth of 1,150 m, the difference between the stresses in foot wall and hanging wall amounts up to 21 MPa. In hanging wall, the value of vertical stresses, while going away from the fault, heads fast for initial values of vertical stresses.

In hanging wall and its direct vicinity, significant stress relief occurs (ratio $\frac{\sigma_z}{p_z}$ equals from 0.1 to 0.20). The range of decompression zone (ratio $\frac{\sigma_z}{p_z}$ between 0.1, and 0.7) amounts to about 220 m near the surface up to about 750 m at a depth of 1,000 m.

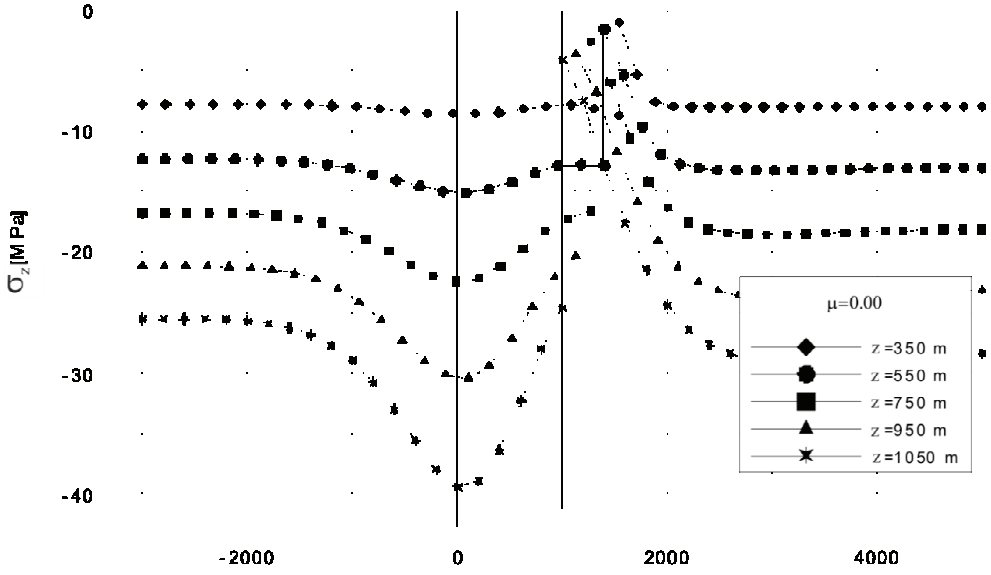

Fig. 3. Distribution of vertical stresses in fault area with inclination 1.5:1 in no friction case

Table 2. Values of vertical stresses in a few places of interest

Inclination of fault 1.5:1 (56.31°), no friction on fault								
Depth H [m]	p_z [MPa]	Zone before fault		On fault				
		$\frac{\sigma_z^{max}}{p_z}$	Distance from fault [m]	σ_z Foot wall [MPa]	$\frac{\sigma_z}{p_z}$ Foot wall	σ_z Hanging wall [MPa]	$\frac{\sigma_z}{p_z}$ Hanging wall	Difference of stresses on fault [MPa]
350	–8.8	1.0	–	–8.9	1.0	–1.0	0.1	–7.0
550	–13.8	1.1	1350	–12.5	0.9	–2.0	0.1	–10.5
750	–18.8	1.2	1200	–17.0	0.9	–3.0	0.2	–14.0
950	–23.8	1.3	1050	–21.0	0.9	–4.0	0.2	–17.0
1150	–28.8	1.4	950	–25.5	0.9	–4.5	0.2	–21.0

In Table 2, values of vertical stresses in a few interesting places are shown.

In Fig. 4, characteristic zones of stress are schematically marked, which can be distinguished in the vicinity of a normal fault (with the inclination 2:1, 63.44°) and the value of friction coefficient: $\mu = 0.0$. In zones "c" and "e", there appear increased horizontal compression stresses, which exceed twice the value of initial horizontal stresses $\frac{\sigma_x}{p_x} > 2.0$. The difference between these zones is that, in zone "e", the ratio of vertical stresses to initial vertical stresses is significantly lower than value 0.7, whereas the same ratio in zone "c" is close to 1.0. Due to that fact, zone "c" can be regarded as dangerous according to the point of view of seismic events and rock bursts. Taking into consideration stress values and the experience gained in mining conditions (rock bursts occur below 500 m), zone "c_1" should be accepted as dangerous, which is located at a depth of about 600 to 950 m and starts at a distance of 700 m from the fault. Description of zones is given in Table 3.

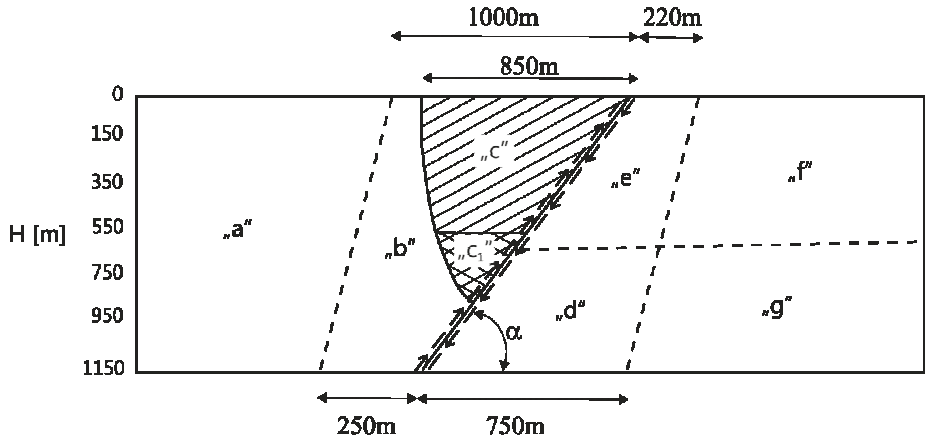

Fig. 4. Characteristic zones of stress

Table 3. Description of the zones

Zones	State of stress		Rockburst hazard in the case of fault vicinity
"a"	$\frac{\sigma_x}{p_x} < 1.3$	$\frac{\sigma_z}{p_z} < 1.3$	Low risk
"b"	$1.3 \le \frac{\sigma_x}{p_x} < 2.0$	$\frac{\sigma_z}{p_z} < 1.3$	Medium risk*
"c"	$2.0 < \frac{\sigma_x}{p_x}$	$\frac{\sigma_z}{p_z} < 1.3$	Heavy risk*
"d"	$\frac{\sigma_x}{p_x} < 1.3$	$\frac{\sigma_z}{p_z} < 0.7$	Low risk, good exploitation conditions
"e"	$1.3 \le \frac{\sigma_x}{p_x} < 1.5$	$\frac{\sigma_z}{p_z} < 0.7$	Low risk, average exploitation conditions**
"f"	$1.3 \le \frac{\sigma_x}{p_x} < 1.5$	$0.7 \le \frac{\sigma_z}{p_z} \le 1.0$	Low risk, average exploitation conditions*
"g"	$\frac{\sigma_x}{p_x} < 1.3$	$0.7 \le \frac{\sigma_z}{p_z} \le 1.0$	Low risk

*As a result of increased horizontal stress, the exploitation should be carried out perpendicular to a fault with a distance equal or higher than 40 m. This should reduce the possible damage inside the longwall panel gateroads.

Calculations done for other inclinations of fault, namely fault with inclinations: 2:1 (63.44°), 3:1 (71.57°), 4:1 (75.96°), 5:1 (78.69°), 6:1 (80.54°), show that both the character of deformation and also the character of disturbance of state of stresses in these models are similar in terms of quality, like in the model discussed above in detail.

In Table 4, values of horizontal stresses are shown in a few chosen places at a depth of 350 m, for different inclinations of the fault.

In Table 5, though, the values of vertical stresses are shown in a few chosen places at a depth of 350 m, for different inclinations of the fault.

The results obtained (Tables 4, 5) show unambiguously that in the case of lacking friction on the fault plane, disturbances in the distribution of stresses and displacements are the higher, the smaller the inclination of fault is.

The calculations carried out above were done with the assumption that there is lack of friction on the fault. Further calculations were done introducing friction of different values on the fault (increasing the value of friction ratio). It was observed that with the increase in friction coefficient μ, the values of compression stresses in the surroundings of the fault de-

Table 4. Values of horizontal stresses in selected places

Depth 350m, $p_x = -2.9$ [MPa], no friction on fault $\mu = 0$							
Inclination of fault	Zone before fault		On fault				
	$\frac{\sigma_x^{max}}{p_x}$	Approximate distance of maximum stresses from fault in [m]	σ_x in foot wall [MPa]	$\frac{\sigma_x}{p_x}$ Foot wall	σ_x Hanging wall [MPa]	$\frac{\sigma_x}{p_x}$ Hanging wall	Difference of stresses on fault [MPa]
1.5:1 (56.31°)	–4.2	1600	–19.5	6.7	–16.5	5.7	–3.0
2:1 (63.44°)	–2.5	1400	–12.0	4.1	–11.5	2.4	–0.5
4:1 (75.96°)	–1.6	1200	–7.0	2.4	–7.0	2.4	0
6:1 (80.54°)	–0.2	1000	–5.0	1.7	–5.0	1.7	0

Table 5. Values of vertical stresses in selected places

Depth 350 m, $p_z = -8.8$ [MPa], no friction on fault $\mu = 0$							
Inclination of fault	Zone before fault		On fault				
	$\frac{\sigma_z^{max}}{p_z}$	Approximate distance of maximum stresses from fault in [m]	σ_z in Foot wall [MPa]	$\frac{\sigma_z}{p_z}$ Foot wall	σ_z Hanging wall [MPa]	$\frac{\sigma_z}{p_z}$ Hanging wall	Difference of stresses on fault [MPa]
1.5:1 (56.31°)	1.0	1470	–8.9	1.0	–1.0	0.1	–7.9
2:1 (63.44°)	1.0	1470	–8.6	1.0	–4.0	0.5	–4.6
4:1 (75.96°)	0.9	1470	–8.2	0.9	–6.9	0.8	–1.3
6:1 (80.54°)	0.9	1470	–8.0	0.9	–7.2	0.8	–0.8

crease heading for the values of initial stresses. For example, at the inclination of fault 1.5:1 (56.31°) at a depth of 350 m:

– for ratio $\mu = 0.0$ on the fault in foot wall $\frac{\sigma_x}{p_x} = 6.7$ and $\frac{\sigma_z}{p_z} = 0.91$,
– for ratio $\mu = 1.0$ on the fault in foot wall $\frac{\sigma_x}{p_x} = 3.3$ and $\frac{\sigma_z}{p_z} = 0.97$.

This observation leads to the conclusion that estimation of friction angle on the fault in connection with its inclination will allow the determination of state of stress increase in the surroundings of the fault, and thereby the degree of danger of seismic events and rock bursts.

It results from the calculations done that with a certain critical value of friction coefficient, dependent on the inclination of the fault plate and strain properties of rocks, relative displacement of the two parts on the fault does not occur.

For each of the inclinations of fault and the accepted strain properties (E = 5.0 GPa, ν = 0.25), after doing variant calculations, critical values of friction coefficient were determined. Depending on inclination angle of the fault, critical value of friction coefficient amounts to:

– inclination of fault 1.5:1 (56.31°) $\mu_{kr} = 2.3$,
– inclination of fault 2:1 (63.44°) $\mu_{kr} = 1.6$,
– inclination of fault 3:1 (71.57°) $\mu_{kr} = 1.05$,
– inclination of fault 4:1 (75.96°) $\mu_{kr} = 0.8$,
– inclination of fault 5:1 (78.69°) $\mu_{kr} = 0.65$,
– inclination of fault 6:1 (80.54°) $\mu_{kr} = 0.54$.

On the basis of that, a very significant conclusion, from a practical point of view, can be formulated, that critical value of friction coefficient, with which mutual displacement of rock mass along the surface of fault does not occur, and the degree of disturbance of state of stress is slight, it is the smaller, the bigger the inclination of fault is.

For the accepted values of mechanical parameters (E = 5.0 GPa, ν = 0.25), the dependence between critical value of friction coefficient and the inclination of fault surface can be approximated with the function in the form

$$\mu_{kr} = \frac{3.3}{\tan \alpha^{1.017}}, \tag{1}$$

with correlation coefficient: $r = 0.998$.

The aim of the next stage of calculations was to check the influence of mechanical parameters on critical values of friction coefficient on the fault surface. For each model with the accepted inclination of fault (1.5:1, 2:1, 3:1, 4:1, 5:1, 6:1), calculations were done, in which the values of Young's modulus were changed (from 2.5 GPa to 40 GPa), and also the values of Poisson's ratio (from 0.15 to 0.45). In total, calculations were done for 256 cases. For each inclination of fault, the results obtained from calculations were approximated with the functional dependence in the form

$$\mu_{kr} = \frac{a \cdot E + b}{\nu} + c \,. \tag{2}$$

For example, for a model with inclination of fault 4:1, the values of equation coefficients (2) were determined by means of non-linear regression method amounted to a = 0.003764, b = 0.30839, c = –0.5239 with correlation coefficient r = 0.991 (Fig. 5).

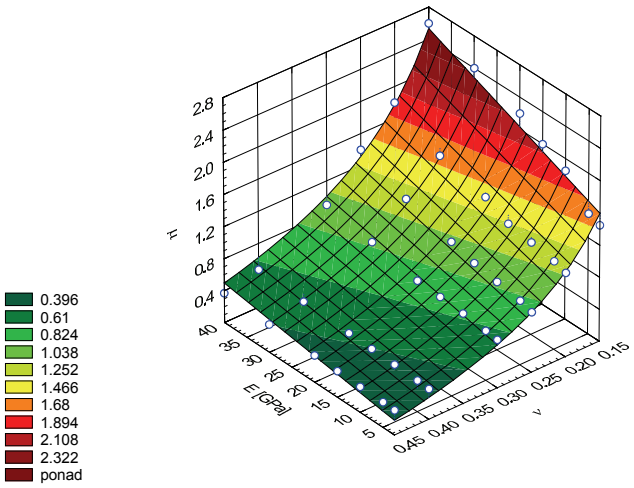

Fig. 5. Approximation results of critical values of friction coefficient calculations for a model with inclination of fault 4:1

Having the results from such a big number of calculations, an attempt was made at their generalization by means of functional dependence (taking advantage of non-linear regression curve) enabling to determine critical values of friction coefficients depending on the inclination of fault surface and mechanical parameters of rock mass. After making a number of attempts and taking into consideration all the results obtained, a dependence was suggested in the form

$$\mu_{kr} = \frac{1}{\tan\alpha}\left[\frac{0.0128 \cdot E + 1.221}{\nu} - 1.935\right], \tag{3}$$

for which the highest correlation coefficient was obtained, which amounts to 0.995j. With these values of internal friction angle, mutual dislocation of rock mass along the fault surface does not occur. In this formula, inclination angle is given in degrees, and Young's modulus in GPa (Flisiak et al. 2000).

In Byerlee's publication (1978), it was presented that three types of friction can be distinguished: initial friction, maximal friction and residual friction. In Poland, rock bursts and seismic events refer to mining of coal and copper ores. Mining does not exceed the depth of 1,250 m, and at this depth initial stresses do not exceed 32 MPa. From Byrlee's research (1978), and also Barton's (1973, 1976), Jaeger and Cook's (1969), Lane and Heck's (1964), Barton and Choubey's (1977) results that up to about 100 MPa, friction along the fault plane (when lack or small width of fault fissure) can be approximated with the dependence (Byerlee, 1978)

$$\tau = 0.85\,\sigma_n \tag{4}$$

where τ, σ_n – stress properly tangential and normal to the fault surface.

Dependence (4) describes maximal friction for different types of rocks, including sedimentary rocks. In the dependence shear stress – normal stresses on the fault for initial friction, the coefficient reaches the values lower than 0.85. Dependence (4) is the upper limit of equations describing initial friction for different rocks.

Accepting $\mu_{\max}$ = 0.85 (equation (4)) and substituting in equation (3), one obtains

$$\alpha_{kr} = \arctan\left[\frac{0.015 \cdot E + 1.436}{\nu} - 2.276\right]. \tag{5}$$

In Fig. 6, dependence of critical value of friction coefficient is schematically presented μ_{kr} from inclination angle of fault plane α for given mechanical parameters E, ν. The marked surface comprises the values of friction coefficients higher than $\mu_{\max}$ = 0.85, with which the slip is possible on the fault plate inclined at angle $\alpha < \alpha_{kr}$.

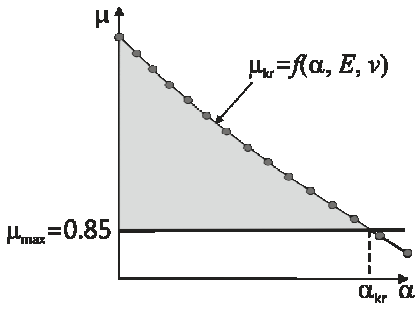

Fig. 6. Dependence of critical value of friction coefficient μ_{kr} on inclination angle of fault plate α

Table 6

Roof rock	Type of mine	R_c [MPa]	E_{sk} [GPa]	ν_{sk} [–]	α_{kr}
Coarse-grained limestone	Coal	46.9	4.86	0.24	76°
Moderately-grained limestone	Coal	54.4	7.21	0.22	78°
Fine-grained sandstone	Coal	68	8.69	0.19	80.5°
Strong fine-grained sandstone	Coal	90	12.00	0.19	80.9°
Coal	Coal	21	2.02	0.3	69°
Limestone, dolomit	Copper ore	108	46.5	0.23	81.9°
Anhydrite	Copper ore	98	55.5	0.26	81.2°

From experience in Polish mines, it is known that the source of seismic events and rock bursts while coal mining are strong sandstones, whereas in copper ore mines, thick layers of anhydrites and limestones. Assuming average parameters for: coarse grained, moderately-grained and fine-grained sandstones, anhydrites, limestones, coal in Table 6, the boundary value of the angle was determined, above which the slip on the fault is not possible. Depending on the kind of rock, it is between 69°, and 81.9°. Whereas in Fig. 7, the change of critical value of internal friction angle is shown, depending on the fault inclination and mechanical properties of the rocks under research.

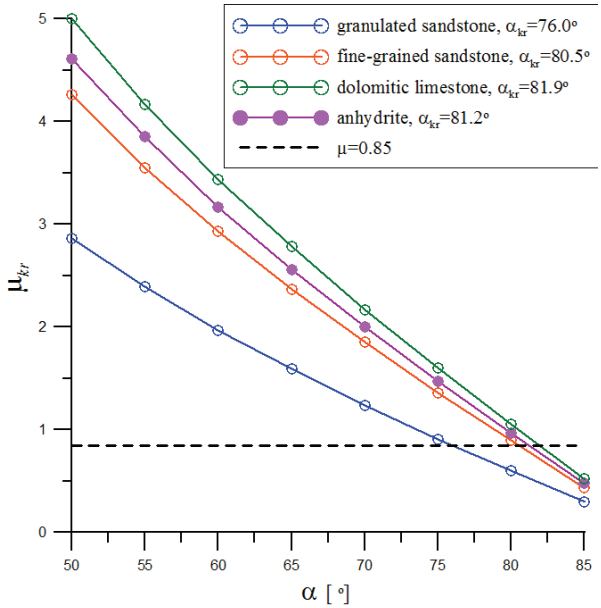

Fig. 7. Influence of fault inclination on critical value of internal friction angle on fault

The problem discussed above is extremely important because there are a lot of faults in the area of Polish mines, which are of local or regional character. It was observed that while mining in the vicinity of faults, especially regional ones, a significant number of seismic events and rock bursts occur. For example, one of such faults is satisfactorily recognized Kłodnicki Fault (Nizicki, Teper, 2002). The fault has a number of branches, accompanying faults and smaller dislocations, but its main part is of normal fault. It is characterized by significant variability of the run and throw changing from about 40 m up to 460 m. It spreads on mining areas of a few Polish mines, from "Sośnica-Makoszowy" Mine to "Wesoła" Mine in the east. General angle of fault surface is between 76° and 85°. The width of fault fissure is variable and is between 4m and 24 m.

Fault fissure is filled with material that comes from destroyed rocks that are in the neighbourhood of fault (refined mudstone, locally mixed with sand and coal dust). Kłodnicki Fault is fundamentally dry. Accepting, for Kłodnicki Fault, friction coefficient $\mu_{max} = 0.85$, it can be observed that boundary value of fault inclination angle for sandstones is included in the range between 76° and 80.5°, which means it is close to the value of general angle of fault surface inclination of Kłodnicki Fault. This leads to the conclusion that rocks in the area of Kłodnicki Fault are in state of unstable equilibrium and while mining in the area of this fault dislocations along the fault surface are possible, which can lead to the occurrence of high-energy seismic events and rock bursts.

3. NUMERICAL CALCULATIONS OF INFLUENCE OF FAULT EXISTENCE ON INITIAL STATE OF STRESS IN ROCK MASS – FAULT MODELLED WITH GOODMAN CONTACT MODELS (GOODMAN ET AL., 1968)

Numerical calculations were done for four models with different dip angle of fault surface (Tajduś et al. 2008; Tajduś et al. 2014):

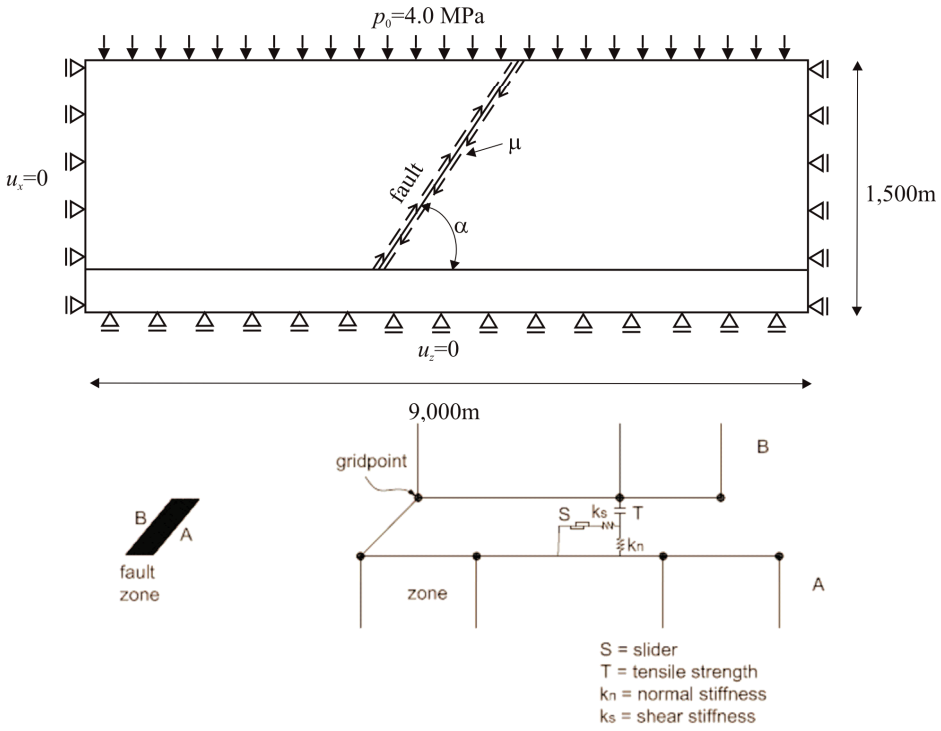

Fig. 8. Calculation plate with Goodman element model

– model 1 – inclination 1.5:1 (56.31°),
– model 2 – inclination 2:1 (63.44°),
– model 3 – inclination 3:1 (71.57°),
– model 4 – inclination 4:1 (75.96°).

In each of the models considered, different values of friction coefficient on fault surface were assumed: $\mu = 0.0$, $\mu = 0.3$, $\mu = 0.5$, $\mu = 1.0$.

A numerical model is shown in Fig. 8.

The upper layer containing the fault is 1200 m thick. The lower layer was introduced in the model as an auxiliary layer of 300 m in thickness in order to avoid concentration of stresses that occur on the contact fault plate with the edge of the plate. On side edges of the plate, zero horizontal displacements were assumed, whereas on the bottom edge of the plate, zero vertical displacements. Interaction of quaternary layers with 160 m thickness was replaced by applying, on the upper edge of the plate, evenly-spread fixed loading of the value of 4.0 MPa.

The plate was covered with a mesh of tetragonal tetra-nodal elements (135,000 elements), whereas the surface of discontinuity was modelled by means of contact elements (Goodman, 1968) of the thickness equal zero enabling independent movement along the fault (slip to each other). In contact elements, stiffness was introduced both on normal direction (k_n) and also shear one (k_s). To limit the shear strength, the Coulomb criterion was used, which determines maximum value of shear strength as a function of normal stress, cohesion and friction of an element. It was assumed that rock mass, in the vicinity of fault, is isotropic and homogeneous in particular layers, and behaves linearly-elastic. Rock mass properties are given in Table 7.

Table 7. Rock mass properties

Young's modulus	E = 5.0 GPa
Poisson's ratio	ν = 0.25
Density	ρ = 0.025 MPa/m^3
Normal stiffness	k_n = 500 MPa/m
Shear stiffness	k_s = 50 MPa/m

For models described above, numerical calculations were done changing both inclination fault angle and also friction coefficient on fault plate beginning with its zero value, for which there was a slip between parts of the model separated by a fault, up to the value of friction coefficient at which a slip did not occur. Because of a big volume of the results obtained, below only some of the results obtained are discussed in detail, and compared with the results obtained for a fault modelled with contact elements GAP.

For model 2 in which fault inclination to horizontal plate amounted to 2:1 (63.44°), calculations were done for the following values of friction coefficient: $\mu = 0.0$, $\mu = 0.3$, $\mu = 0.5$, $\mu = 0.6$. The analysis of the results obtained indicates that the highest disturbances of state of stress and displacement appear in

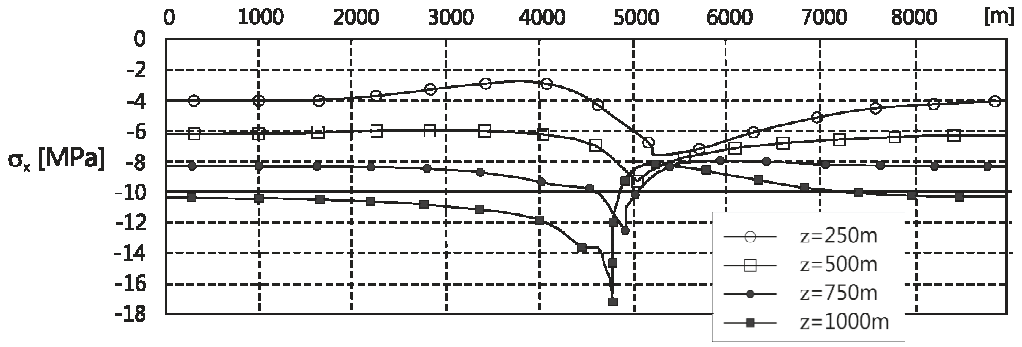

Fig. 9. Distribution of horizontal stresses (model 2, inclination of fault 2:1, $\mu = 0.0$)

rock mass where on the surface of the fault friction (μ = 0.0) does not occur, as the friction values increase, the disturbance caused by the fault existence decreases and with friction value μ = 0.6 a slip on the fault does not occur and disturbance of initial state of stress is small. In Fig. 9, distribution of horizontal stresses at a few depths: 410 m, 660 m, 910 m, 1160 m is shown. The distribution of these stresses differs a little from the ones obtained before (contact elements GAP on the fault). In this case, *in foot wall* while coming closer to the fault, the compression values of horizontal stresses increase and they reach the highest compression values on the fault. After crossing the fault, *in foot wall* the values of decompression stresses decrease and then while going further from the fault, they head for the values of horizontal initial stresses. Rapid decrease in horizontal stresses on the fault is not observed, as in the case when contact element GAP are used on the fault.

In Table 8, maximum values of horizontal compressive stresses on the fault for three values of friction coefficient $\mu = 0.0$, $\mu = 0.3$, $\mu = 0.5$ are given.

Table 8

Inclination of fault 2:1 (63.44°)							
Depth H [m]	p_x [MPa]	on fault					
		$\mu = 0.0$		$\mu = 0.3$		$\mu = 0.5$	
		σ_x [MPa]	$\frac{\sigma_x}{p_x}$	σ_x [MPa]	$\frac{\sigma_x}{p_x}$	σ_x [MPa]	$\frac{\sigma_x}{p_x}$
410	–3.4	–7.5	2.2	–6.7	2.0	–3.7	1.1
660	–5.5	–9.3	1.7	–7.3	1.3	–5.8	1.1
910	–7.6	–12.7	1.7	–9.3	1.2	–8.0	1.1
1160	–9.7	–16.8	1.7	–12.5	1.3	–10.2	1.1

From the distribution of vertical stresses shown in Fig. 10, it follows that in the whole analysed model these stresses are of compressive character. Similarly as in the case of horizontal stresses *in foot wall*, while coming closer to the fault, compressive values of vertical stresses increase and they reach the highest compressive values on the fault. After crossing the fault, *in foot wall*, the values of compressive stresses decrease, and then while going further from the fault they head for the values of vertical initial stresses.

In Table 9, maximum values of vertical compressive stresses on the fault are given, for two values of friction coefficient μ = 0.0, μ = 0.3. As can be observed in foot wall of the fault, there is a relatively small increase in compressive stresses (in the vicinity of the fault plate), whereas just behind the fault in hanging wall, there is a significant decrease in compressive stresses, decompression occurs. Compressive stresses fall to the values from $0.5p_z$ to $0.8p_z$, and then gradually increase up to the values of vertical initial stresses p_z. Depending on the depth, decompression zone behind the fault in hanging wall can be estimated from 50–100 m at small and medium depth, up to 600–800 m at big depths.

In model 2 (inclination of the fault 2:1, 63.44°) with contact elements Goodman, critical value of friction coefficient on the fault amounts to μ_{kr} = 0.6, whereas contact elements GAP type are used, critical value of friction coefficient on the fault amounts to μ_{kr} = 1.6. It shows how important the way of the fault modelling is.

It can be said that the usage of Goodman contact elements can reflect, in a better way, real model of a fault with a big throw with deformation ability of rock mass surfaces (they are characterized with parameters k_n and k_s). There is often breccia zone between them, which is characterized by small values of mechanical properties. That is the matter for further research and numerical simulations, assuming even the use of the most popular Coulomb–Mohr elastic-plastic model for breccia.

It follows from the analysis of main stresses in the vicinity of faults that their values differ from a few to dozen or so percent in comparison with stress values σ_x, σ_z.

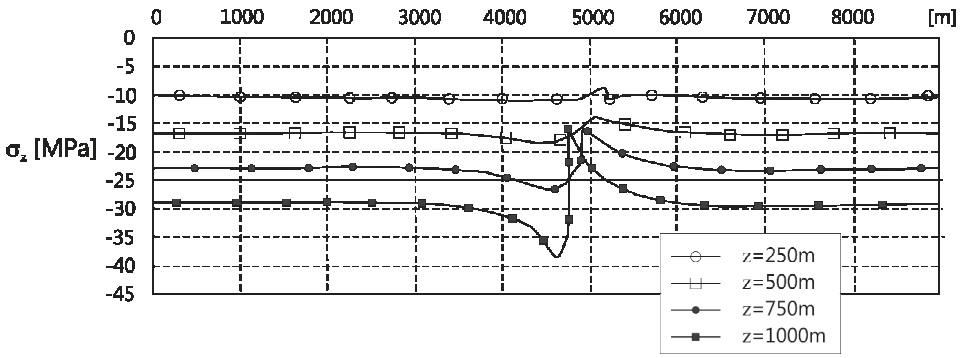

Fig. 10. Distribution of vertical stresses (model 2, $\tan\alpha = 2.0$; $\mu = 0.0$)

Table 9

Inclination of fault 2:1 (63.44°)									
Depth H [m]	p_z [MPa]	On fault							
		$\mu = 0.0$				$\mu = 0.3$			
		Foot wall		Hanging wall		Foot wall		Hanging wall	
		σ_z [MPa]	$\frac{\sigma_z}{p_z}$	σ_z [MPa]	$\frac{\sigma_z}{p_z}$	σ_z [MPa]	$\frac{\sigma_z}{p_z}$	σ_z [MPa]	$\frac{\sigma_z}{p_z}$
410	–10.25	–10.6	1.0	–8.2	0.8	–10.3	1.0	–9.3	0.9
660	–16.5	–18.5	1.1	–13.7	0.7	–17.9	1.1	–12.9	0.8
910	–22.75	–26.5	1.2	–14.6	0.6	–24.3	1.1	–19.0	0.7
1160	–29.0	–38.0	1.3	–15.5	0.5	–33.6	1.2	–20.7	0.7

For model 4, in which inclination of the fault to horizontal plate amounted to 4:1 (75.96°), calculations were done for the following values of friction coefficient: $\mu = 0.0$, $\mu = 0.2$, $\mu = 0.3$. Similarly as before, the biggest disturbance of state of stress and displacement occurs in rock mass, in which friction ($\mu = 0.0$) does not occur on the fault surface, as the friction values increase, the disturbance caused by fault existence decreases and with friction value $\mu = 0.3$ a slip on the fault does not occur.

In *foot wall*, the closer to the fault, the values of compressive horizontal stresses increase and they reach the biggest values on the fault. After crossing the fault in *hanging wall* the values of compressive stresses decrease, and then the further from the fault, they head for the values of horizontal initial stresses.

In Table 10, values of maximum horizontal compressive stresses on the fault are given, for three values of friction coefficient $\mu = 0.0$, $\mu = 0.2$, $\mu = 0.3$.

From the distribution of vertical stresses, it follows that in the whole analysed model these stresses are of compressive character. Similarly to the case of horizontal stresses in *foot wall*, the closer to the fault, the values of compressive vertical stresses increase and reach the biggest compressive values on the fault. After crossing the fault in *hanging wall*, the values of compressive stresses decrease, and then the further from the fault, they head for the values of vertical initial stresses. In Table 11, maximum values of vertical compressive stresses on the fault are given, for two values of friction coefficient $\mu = 0.0$, $\mu = 0.2$.

Table 10

Inclination of fault 4:1 (75.96°)							
Depth H [m]	p_x [MPa]	On fault					
		$\mu = 0.0$		$\mu = 0.2$		$\mu = 0.3$	
		σ_x [MPa]	$\frac{\sigma_x}{p_x}$	σ_x [MPa]	$\frac{\sigma_x}{p_x}$	σ_x [MPa]	$\frac{\sigma_x}{p_x}$
410	–3.4	–5.3	1.6	–4.1	1.2	–3.4	1.0
660	–5.5	–6.8	1.2	–5.9	1.1	–5.6	1.0
910	–7.6	–9.1	1.2	–8.0	1.1	–7.7	1.0
1160	–9.7	–11.6	1.2	–10.6	1.1	–9.9	1.0

Table 11

Inclination of fault 4:1 (75.96°)									
Depth H [m]	p_z [MPa]	On fault							
		$\mu = 0.0$				$\mu = 0.2$			
		Foot wall		Hanging wall		Foot wall		Hanging wall	
		σ_z [MPa]	$\frac{\sigma_z}{p_z}$	σ_z [MPa]	$\frac{\sigma_z}{p_z}$	σ_z [MPa]	$\frac{\sigma_z}{p_z}$	σ_z [MPa]	$\frac{\sigma_z}{p_z}$
410	–10.25	–10.8	1.1	–9.7	0.9	–10.5	1.0	–9.8	1.0
660	–16.5	–17.4	1.1	–14.9	0.9	–17.2	1.0	–15.5	0.9
910	–22.75	–25.2	1.1	–18.7	0.8	–23.7	1.0	–20.1	0.9
1160	–29.0	–35.1	1.2	–20.1	0.7	–32.9	1.1	–23.3	0.8

In foot wall in the vicinity of the fault, there is a small increase in compressive stresses, whereas just behind the fault in hanging wall there is a decrease in compressive stresses. Compressive stresses fall to the values from $0.9p_z$ to $0.7p_z$, and they gradually increase up to the values of vertical initial stresses. Depending on the depth, the decompression zone behind the fault in hanging wall can be estimated from 20–50 m at small and medium depths, up to 400–600 m at big depths. The values of principal stresses were also determined in calculations. From the analysis of the values of main stresses σ_1, σ_2 in the vicinity of faults, it follows that their values differ in comparison with the values of stresses σ_x, σ_z.

In model 4 (inclination of fault 4:1, 76.96°) with Goodman contact elements, critical value of friction coefficient on the fault amounts to $\mu = 0.3$, whereas contact elements GAP type are used, critical value of friction coefficient on the fault amounts to $\mu = 0.8$.

4. CONCLUSIONS

On the basis of the calculations and analyses done, the following conclusions can be formulated:

- results of calculations of state of stress in the vicinity of the normal fault depend on the way of fault plane modelling. Comparison of the two ways of fault plane modelling (with contact elements GAP type, or Goodman contact elements) indicates that contact elements GAP type describe better the behaviour of fault with small thickness of fault fissure;
- discontinuity existence in rock mass causes significant disturbance in the distributions of stresses and displacements;
- in foot wall, the degree of disturbance is significantly higher than in hanging wall;
- decisive factor about the size of disturbance are the conditions that appear on the contact between foot wall and hanging wall. For a fault with determined geometry and mechanical properties, there is a certain critical value of friction coefficient, above which a slip of the contacting with each of the other parts of rock mass is impossible. With the values of friction coefficient smaller than critical one, the degree of disturbance is the bigger, the smaller the value of this coefficient is;
- the value of critical friction coefficient depends on inclination angle of fault surface and mechanical properties;
- in rock mass of the same elastic properties of rocks, critical friction coefficient is in inverse proportion to the inclination of fault;
- for faults with the same inclination, critical friction coefficient, which is responsible for the degree of disturbances, is in direct proportion to the value of Young's modulus and inversely proportional to Poisson's ratio. Therefore, it can be said that as far as friction coefficient on contact is an objective quantity, then in rock mass with higher mechanical parameters, the degree of disturbance is significantly higher than in rock mass whose parameters have lower values. This conclusion is confirmed by numerous observations made while mining in real conditions, which indicates that occurrence of layers of strong sandstones with high value of Young's modulus and small value of Poisson's ratio in rock mass, contribute to significant growth of high energy seismic events and rock bursts hazard;
- change of conditions on contact, which consists in friction coefficient decrease, for example, due to rock mass hydration, irregular mining on both sides of the slope, can lead to significant deterioration of mining and growth of seismic events and rock bursts hazard;
- dependences obtained enable prediction of the conditions for mining in the vicinity of faults on condition that the geometry of a fault is known,

values characteristic of friction and mechanical properties of rock mass.

REFERENCES

[1] BYERLEE J., *Friction of Rocks*, Birkhauser Verlag, Pageoph., 1978, Vol. 116, 615–626.

[2] BARTON N.R., *Review of a new shear strength criterion for rock joints*, Engng. Geol., 1973, 7, 287–332.

[3] BARTON N.R., *The shear strength of rock and rock joints*, Int. J. Rock Mech. Min. Sci. & Geomech. Abstr., 1976, 13, 1–24.

[4] BARTON N.R., CHOUBEY V., *The shear strength of rock joints in theory and practice*, Rock Mech. 1977, 10, 1–54.

[5] JAEGER J.C., COOK M.G.W., *Fundamentals of Rock Mechanics*, London 1969.

[6] LANE K.S., HECK W.J., *Triaxal testing for strength of rock joints*, Proc. 6th Symp. Rock Mech. Rolla, 1964, 98–108.

[7] FLISIAK J., TAJDUŚ A., CAŁA M., FLISIAK D., *Geomechaniczne zjawiska wywołane eksploatacją w górotworze zaburzonym tektonicznie*, (*Geomechanical phenomena due to mining excavation in tectonically engaged rock mass*), Scientific project No. 9T12A01112, (in Polish, unpublished).

[8] TAJDUŚ A., FLISIAK J., CAŁA M., *Wpływ pierwotnego stanu naprężenia w górotworze na zagrożenia tąpaniami*, (*Interaction of initial stress field with rockburst hazard*), Materiały konferencji Tąpania 2004, Ustroń–Katowice, 2004, 325–356.

[9] TAJDUŚ A., FLISIAK J., CAŁA M., (2008–2011): *Numeryczna analiza stanu zagrożenia tąpaniami w rejonie zaburzeń tektonicznych*, (*Numerical analyses of rockburst's hazard in tectonic zones*), Scientific project No. N N524 376 234, (in Polish, unpublished).

[10] TAJDUŚ A., CIEŚLIK J., TAJDUŚ K., *Rockburst hazard assessment in bedded rock mass. Laboratory tests of rock samples and numerical calculations*, Archives of Mining Science, 2014, Vol. 59, Issue 3, 591–608.

[11] GOODMAN R.E., TAYLOR R.L., BREKKE T.L., *A model for the mechanics of jointed rock*, J. Soil Mech. Foundations Div., 1968, 99, 637–659.

[12] NIZICKI R., TEPER L., *Przebieg i wykształcenie strefy uskokowej uskoku kłodnickiego w OG KWK Halemba*, (Geological origin of Kłodnicki fault zone in OG KWK Halemba), Mat. XXV Symp. Geologia Formacji Węglonośnych Polski, Wyd. AGH, Kraków, 2002, 115–121, (in Polish).